Optimization of the Production of Epichlorohydrin Catalyzed by TS-1 Using the Taguchi Method

Rui Pan, Rumeng Jiang, Yao Chen and Jiancheng Zhou*
School of Chemistry and Chemical Engineering, Southeast University, Nanjing, 211189, P.R. China.
jczhou@seu.edu.cn*

Summary: Mass production of Epichlorohydrin (ECH) via epoxidizing allyl chloride suffers from determining the optimal reaction parameters and reproducibility. Titanium silicalite-1 (TS-1) catalyst has been successfully employed to reduce activation energy, but many reaction conditions are involved in the process. To optimize ECH production by analysing its yields, Taguchi method was implemented for reducing time and cost. Included in the reaction parameters were reaction temperature, reaction time and the reactant ratio. This study investigated preparation of heterogeneous catalysts using hydrothermal method and their characterization by XRD, IR, SEM and TEM, which confirmed the presence of ordered MFI structure. Plots of S/N suggested that reaction time was the most influential factor, followed by reaction time in ECH production. The optimum factor parameters were acquired as follows, a reaction time of 40 min, reaction temperature of 90 $^{\circ}$C and the molar ratio of H_2O_2: allyl chloride equal to 1. Aimed at the final confirmation, ECH production experiment was also practiced. Established on the obtained results, the yield of ECH was hugely upgraded to the value of 83.13 ± 1.03 % with only ~0.7% deviated from predicted value.

Keywords: Epichlorohydrin; Titanium silicalite-1; Optimization; Taguchi method.

Introduction

Epichlorohydrin (ECH), a colorless, volatile oily liquid, one of the most crucial organic synthetic intermediates, is applied extensively in the industrial manufacture from production of epoxide resins, chlorohydrin rubbers [1-4], several pharmaceutical products, CO_2 reutilization to functionalization material [5-9]. There have been several industrial synthesis approaches recorded for the manufacture of ECH from propylene chlorination [10-12], glycerol chlorination [13], to propylene acetate hydrolysis. Among these routes, the chlorination of propylene under high temperature is more widely used, deriving benefit from its lower fixed-asset investment and abundant raw material storage. However, it brings about high consumption of energy and chlorine as well as the emergence of many by-products which need to be purified further and cause severe environment hazards.

In recent years, to achieve the requirement of green chemistry and sustainable economy, the expansions of alternative environmentally-begin synthetic and lucrative routes are of primary concern. To obtain high atom efficiencies and low E-factor, varieties of novel methods were studied for synthesis of ECH particularly epoxidation of allyl chloride (AC) especially the process catalyzed in liquid phase employing dilute hydrogen peroxide as oxidant [14,15]. Compare with traditional production process,

heterogeneous catalyst supported by titanium-containing zeolites or molecular sieves, for instance, TS-1, Ti-Beta, and Ti-MWW, has shown significant advantages with benefit in the decrease of pollution, energy-efficient and mild operation conditions [16]. However, considering their deficiency in oxidation ability and hydrothermal stability with respect to TS-1 and Ti-Beta, the rest titanium materials are unsatisfactory catalysts for the epoxidation. Diverse catalysts were applied to this reaction [17], among which TS-1 is the most commonly competitive catalyst owing to its strong oxidization ability to transform substantial organic compounds, including olefins, alkanes, phenols and alcohols under mild conditions [18,19]. However, TS-1 was generally prepared through complex methods in which the template was unaffordable [20], during which some unwanted anatase (TiO_2) was formed. Additionally, the selectivity for ECH is unsatisfactory and need to be improved further. The raw material for synthesis of catalyst is silica solution and tetrapropylammonium bromide (TPABr), instead of expensive tetraethyl orthosilicate and tetrapropylammonium hydroxide (TPAOH), which can greatly reduce the production cost of catalyst, and promote the industrial application of TS-1 molecular sieve [21, 22], furthermore propylene epoxidation was selected as probe reaction to investigate the impact of synthesis conditions to the activity of TS-1 and the parameters were optimized.

---

*To whom all correspondence should be addressed.

Nevertheless, the yield of ECH in this route was affected by numerous factors, thus an appropriate design of experiment was required.

In order to obtain optimum process factors, a systematic study to this process is needed. Generally, experimental methods designed in traditional way are facing inconvenience and complexity. Moreover, massed experiments have to be performed when affecting procedure factors are huge. On account of these difficulties, the Taguchi method, an influential tool was proposed in the late 1960s to design high quality systems [23, 24]. With this method, statistical and ideal results were obtained that were similar to those obtained through a full-factorial design, but required fewer experiments and shorten the experiment time. Taguchi method have been shown, in the research and development stage, to be an effective method for improving productivity by bringing along low costs and high-quality products [25, 26]. Using a specially designed orthogonal array, we extensively analyzed the parameter space. The signal-to-noise (S/N) ratio was proposed as a useful metric to discuss the deviate degree of quality characteristics and their desired values, and the experimental data corresponding to each combination of conditions was then transformed into S/N ratio. L_9 OA was employed to identify the optimized levels of the process factors. As well as S/N ratio analysis, a statistical analysis of variance (ANOVA) was conducted to identify statistically significant process factors. With both S/N ratio analysis and ANOVA analysis, the best process parameters could be determined precisely. Finally, a test must be conducted to confirm the elements of optimal synthesis that were discovered by the Taguchi method. A large number of applications of Taguchi method have been achieved in various fields in a wide range of industries because of the high level of interest generated by the Taguchi method [27, 28]. Based on our understanding, there is no detailed study reported L9 OA optimization for using TS-1/SiO$_2$ catalyzing ECH production. As a result, the objective of the present study is to identify the ideal reaction parameters: the reaction time, reaction temperature, as well as molar ratio of H$_2$O$_2$. As a result of considering both the signal-to-noise ratio (S/N) and variance (ANOVA) when optimizing the ECH yield parameters, the most effective parameters were determined.

Experimental

Synthesis of ECH

ECH was synthesized in the home-made water bath setup Fig1: 150 mL round-bottom flask, thermometer, and magnetic stirrer. To the reactor, 2 ml of 30 wt% H$_2$O$_2$ was added, along with a small amount of methanol, allyl chloride and 0.5 g of TS-1. The quantity of residual H$_2$O$_2$ was titrated by iodometric reaction. The analysis of target product ECH applied a gas chromatograph (Shimadzu GC-2014). The conversion rate of allyl chloride (X$_{AC}$), selectivity of epichlorohydrin (S$_{ECH}$) and yield of epichlorohydrin (Y$_{ECH}$) were calculated with the following equations.

$$X_{AC} = \frac{n_{AC}^0 - n_{AC}}{n_{AC}^0}, \quad S_{ECH} = \frac{n_{ECH}}{n_{AC}^0 - n_{AC}}, \quad Y_{ECH} = X_{AC} \times S_{ECH},$$

where $n^0{}_{AC}$ and n_{AC} are the molar quantity of AC before and after the reaction, accordingly n_{ECH} means the final quantity of ECH.
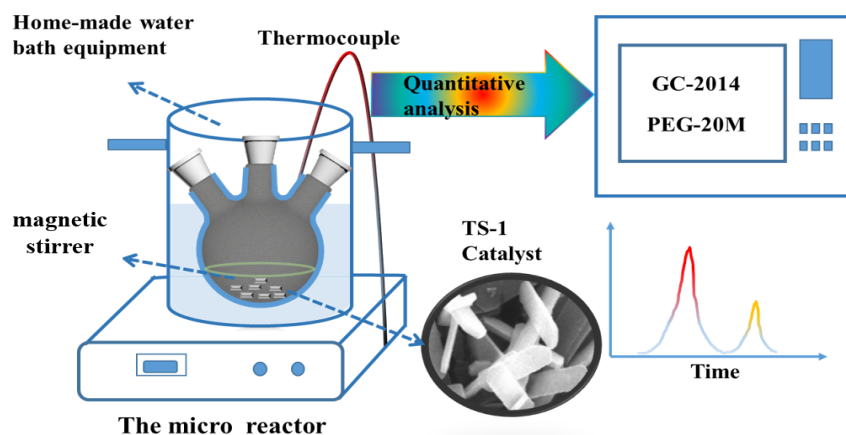

Fig. 1:   Schematic illustration of experimental setup.

Synthesis of TS-1

Catalyst TS-1 synthesis: First, 180 mL deionized water was added to a 250 mL flask and cooled to ~0 °C in an ice water bath. Then 1.7 mL tetrabutyl titanate was quickly dropped into the solution and stirred vigorously for 1h. Next, 5 mL H_2O_2 was added to the above solution and stirred for 1 h. 123 mL of n-butylamine was added to the solution and stirred for 3.5 h. The above operation is the preparation of A solution system. 56 mL silica solution (SiO_2 25 wt%) was added to a 250 mL flask, followed by 100 mL deionized water and 10 g tetrapropyl ammonium bromide stirred at room temperature (25 °C) for 1 h. This operation is the preparation of B solution system. Next, the prepared solution of A was added drop by drop into solution of B at 80 °C, and then stirred for 30 minutes. Then the mixture was heated to 100 °C for reflux for 12h, and then transferred to the 1000 mL high temperature autoclave for crystallization at 170 °C for 72h. The reacted solution was centrifuged and then the resulting solids were washed three times with water and ethanol, respectively. The obtained solids were dried at 120 °C for 24 hours. The final catalyst was prepared by calcination at 550 °C for 6 hours in muffle furnace.

Characterization

X-ray powder diffraction (XRD) pattern of the TS-1 catalyst was obtained by a Bruker D8-Discover diffractometer. The Fourier transform infrared (FTIR) spectrum was acquired on a Thermo Nicolet 5700 spectrometer. The scanning electron microscope (SEM) micrograph was obtained on a FEI Inspect F50 electron microscope with an operating voltage of 15 kV and a FEI Tecnai G2 F20 transmission electron microscope (TEM) was used to investigate the microstructure of the catalyst. Nitrogen adsorption-desorption measurement was carried out on a Micromeritics ASAP 2020 HD 88 nitrogen adsorption apparatus after the TS-1 catalyst was degassed at 120 °C for 6 h. The specific surface area and average pore diameter was calculated by the Brunauer-Emmett-Teller (BET) and Barrett-Joyner-Halenda methods. The total pore volume was dependent on the absorbed N2 volume at a relative pressure of approximately 0.98.

During the epoxidation of allyl chloride, the product (Epichlorohydrin), byproducts (E:1-chloro-3-methoxy-2-propanol and CG:3-chloro-1, 2-propylene glycol) and raw materials (Allyl chloride) were analyzed by gas chromatography. Gas chromatographic analysis conditions were as follows: Chromatographic model: Shimadzu GC-2014; Column: OV-1701 30 m × 0.25 mm × 0.33 μm; Detector: Hydrogen flame ion detector (FID); Detector temperature: 250 °C; Vaporization chamber temperature: 240 °C; The column temperature program was 40 °C, kept for 3 min, 20 °C min^{-1} heated to 130 °C, and kept at 130 °C for 2 min. Nitrogen partial pressure: 350 kPa; Air partial pressure: 240 kPa; Partial pressure of hydrogen: 170 kPa; Injection volume: 0.2 μL.

Taguchi orthogonal experimental design

Orthogonal experimental design was initiated to minimize experiment number and optimize ECH synthetic parameters. Three controllable process parameters have been selected at three levels in Table 1, i.e., reaction temperature, reaction time and molar ratio of H_2O_2 to AC, based on reported related reaction parameters in the literature [18, 29, 30].

Table-1: Factors and their levels under investigation.

Symbol	Factor	Level	Level	Level
A	Reaction temperature (°C)	40	45	50
B	Reaction time (min)	60	90	120
C	Molar ratio of H_2O_2 to AC	1.0	1.2	1.4

Each experiment was repeated three times to investigate the effects of uncertain elements. To use the Catalyst for subsequent cycling, it was washed with ethanol and water and dried at 60 °C overnight. A L_9 orthogonal array with condition combinations as given in Table-2. This array was adequate to handle three-level process factors with eight degrees of freedom. There are four columns in the L9 orthogonal array, and one is vacant for the experiments error. Using the Taguchi method, the yield of ECH was considered the most important quality criterion.

Table-2: Experimental layout using the $L_9(3^4)$ orthogonal array.

	Factor and level			
Trial no.	A	B	C	Error
T1	40	60	1.0	1
T2	40	90	1.2	2
T3	40	120	1.4	3
T4	45	60	1.4	2
T5	45	90	1.0	3
T6	45	120	1.2	1
T7	50	60	1.2	3
T8	50	90	1.4	1
T9	50	120	1.0	2

Results and Discussion
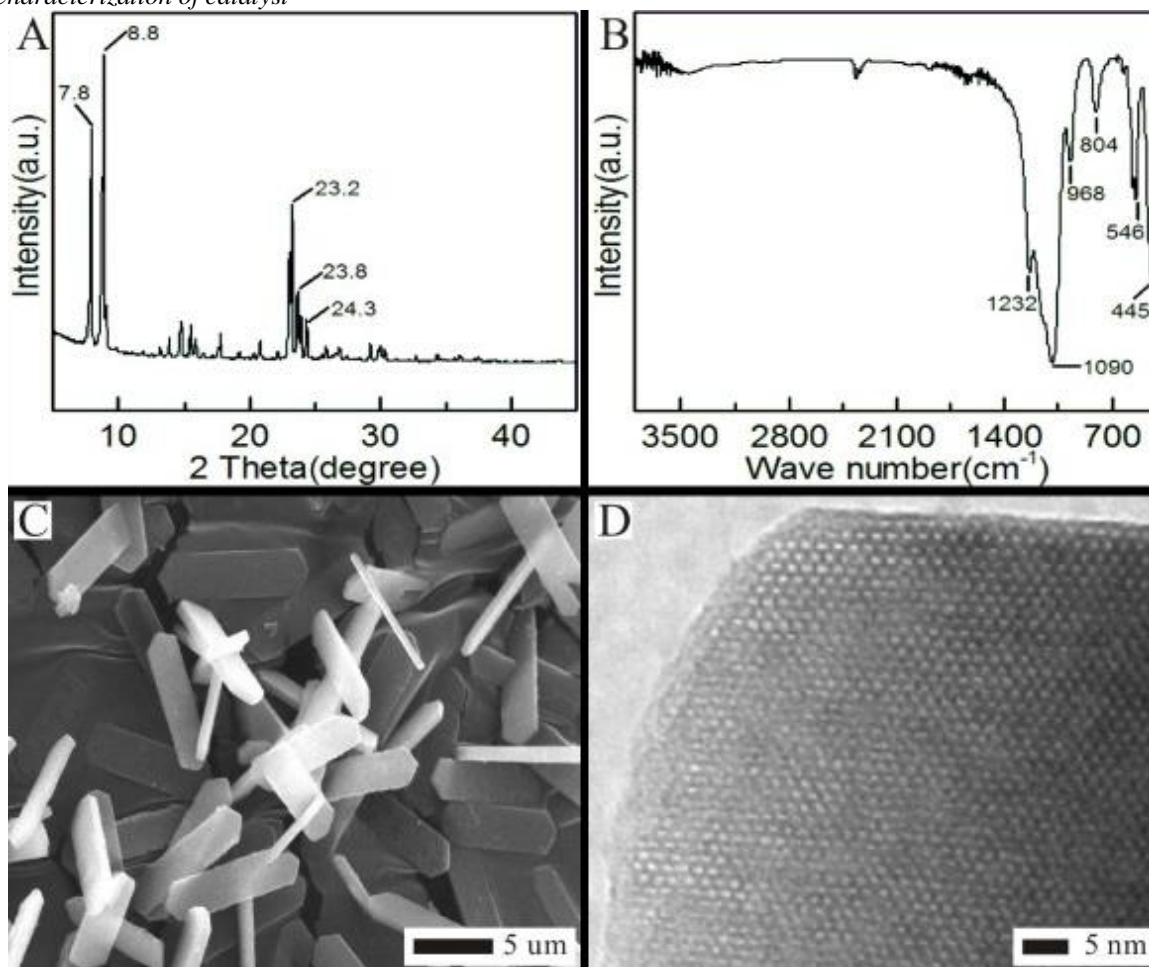
Characterization of catalyst

Fig. 2:   A) XRD patterns, B) FT-IR spectra of TS-1, C) SEM image of TS-1, D) TEM image of TS-1.

Fig 2A shows the powder pattern taken by X-rays for the TS-1. Several characteristic peaks appear at 7.8°, 8.8°, 23.2°, 23.8°, and 24.3° in the same pattern as reported widely in literatures, thus confirming the MFI's topology [31-33]. A peak at 25.4° was also not observed, hinting at only a trace amount of Ti being formed as anatase phase. As well as FTIR analysis, TS-1 samples (Fig 2B) were also analyzed. On the basis of these spectra, the main absorption bands occur at around 450, 550, 800, 1100, 1220 cm^{-1} for this sample, which is consistent with what has been reported in the literature for TS-1 FTIR spectra [34,35]. Ti atoms tetrahedrally coordinate within the silicalite framework as indicated by the band at ~960 cm-1, whose intensity is directly proportional to titanium abundance [36]. SEM images of the samples given in Fig 2C exhibit similar hexagonal prism morphologies and uniform crystallite size distribution of TS-1. The TEM picture of TS-1 at high resolution is shown in Fig 2D, and through this image the uniform pore structure is visible, confirming that the incorporation of Ti does not alter the Si-O structure significantly.TS-1, synthesized in accordance with the above results, was successfully doped with Ti atoms into the Si-O framework. The N$_2$ adsorption-desorption isotherm (the red line) and pore size distribution curve of TS-l was shown in Fig 3. The TS-1 catalyst exhibited Langmuir type-Ⅳ isotherm with a hysteresis loop, which was the characteristic feature of mesoporous material. In addition, the pore size distribution confirmed the presence of mesoporous structures and micropores. The BET surface area, pore volume and pore diameter of TS-1 catalyst were 398.8 m^2/g, 0.282 m^3/g and 3.641 nm,

respectively. A large improvement in production yield can be achieved by optimizing the synthetic factors by using the experimental results presented in Table-3 as a measure. These experimental results indicate that relatively significant effect is seen of procedure parameters on the yield of ECH. In addition, the conversion rate of raw material allyl chloride, selectivity of target product epichlorohydrin, and selectivity of by-products 1-chloro-3-methoxy-2-propanol and 3-chloro-1, 2-propylene glycol were shown in Table-4.
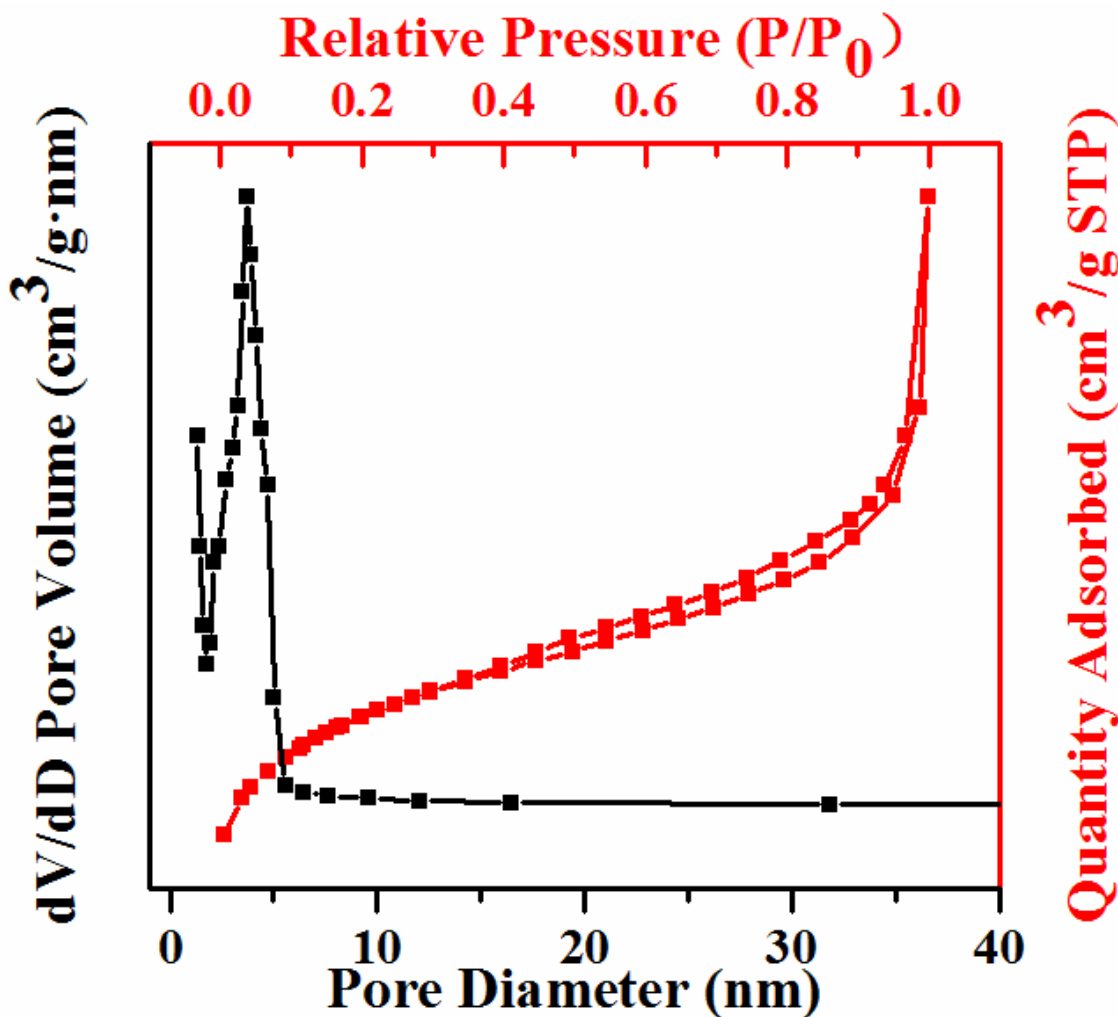

Fig. 3: N_2 adsorption-desorption isotherm (the red line) and pore size distribution curve of TS-l.

Table-3: Experimental results for the yield of ECH and corresponding S/N ratio.

Trial no.	Reaction Temperature(ºC)	Reaction time(min)	Molar ratio of H_2O_2 to AC	Yield (%)	S/N ratio (dB)
1	40	60	1	64.3±2.78	-3.832
2	40	90	1.2	68.4±2.25	-3.300
3	40	120	1.4	73.1±1.99	-2.717
4	45	60	1.2	72.2±2.08	-2.835
5	45	90	1.4	79.1±1.32	-2.032
6	45	120	1	81.0±1.25	-1.827
7	50	60	1.4	64.8±2.62	-3.770
8	50	90	1	77.3±1.44	-2.242
9	50	120	1.2	79.3±1.33	-2.012

[a] Standard uncertainty in the yield of ECH are reported following ± signs. The values are obtained at least three measurements at each condition.

Analysis of the S/N ratio

With Taguchi method, the ratio of the effects of each operational variables (mean value) to the response to them (SD) is computed as the signal-to-noise (S/N) ratio. In accordance with the input desired value, the S/N proportion measures the output quality [23, 24]. The S/N proportion, noted as η, can be acquired from Eq. (2).

$$\eta = - \cdot \log(M.S.D.) \quad (2)$$

For evaluating the effect of process parameters on product properties, a logarithmic function of M.S.D. value was used. Accordingly, higher-the-better quality type M.S.D. can be calculated.

$$M.S.D. = \frac{1}{r}\sum_{i=1}^{r} \frac{1}{y_i^2} \quad (3)$$

While quality characteristic of lower-the-better type can be stated as the following:

$$M.S.D. = \frac{1}{r}\sum_{i=1}^{r} y_i^2 \quad (4)$$

In Eq. (3) and Eq. (4), y_i represents the experimental output, and r stands for repetition number done for each experiment in the orthogonal design.

Obviously, to obtain optimal ECH synthesis factors, the former analytic method for the yield of ECH should be applied. Therefore, Eq. (2) and Eq. (3) were applied to determine the yield of ECH after computing the S/N ratios; in this case, in Table 3, the results of r refer to unity, and they were listed in the last column.

Benefiting from the orthogonal experimental designation, outstanding the effect of individual procedure parameter at various levels is fairly practical. The mean S/N ratio for the reaction temperature at levels 1, 2, and 3, for instance, can be calculated by taking the average of each experiment's S/N ratio during the first three experiments. By applying this method to all levels, we can calculate the S/N for each level of the other process as well. Consequently, as given in Table 5, a relevant S/N table was obtained. Additionally, Fig 2 illustrated the corresponding trend of $\overline{\eta}$, the total mean S/N ratio for the nine experiments.

Closer value will come to the desired output characteristic with higher S/N ratio, and therefore the better-quality characteristic will be. Accordingly, levels with the highest S/N ratio are commonly the most efficient [23, 24]. After digging into Table 5 and Fig 4, following are the optimal factor levels for maximizing ECH yields: reaction temperature (level 1), reaction time (level 2), and molar ratio of H_2O_2 to AC (level 1), which can be denoted as A1B2C1. To determine the optimal combination of parameters levels more accurately, the relative significance among three process factors which were chosen required to be Figd out.
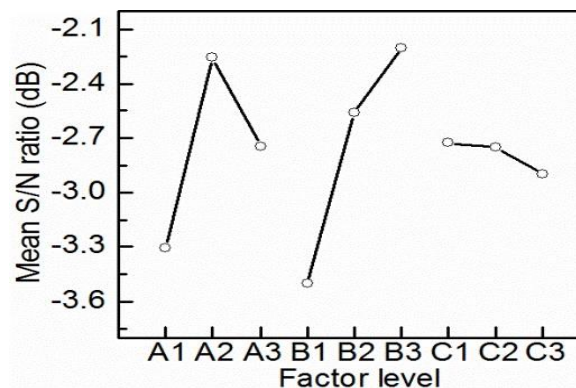

Fig. 4:   S/N graph for the yield of ECH.

Table-4: Conversion of raw material allyl chloride and selectivity of reaction products

Trial no.	Conversion of Allyl chloride $C_{(AC)}$ %	Selective of Epichlorohydrin $S_{(ECH)}$ %	Selective of 1-chloro-3-methoxy-2-propanol $S_{(E)}$ %	Selective of 3-chloro-1, 2-propylene glycol $S_{(CG)}$ %
1	66.2	97.2	No detection	2.8
2	74.0	92.4	0.7	6.9
3	80.6	90.7	1.9	7.4
4	75.3	95.9	1.6	2.5
5	89.8	88.1	4.3	7.6
6	93.2	86.9	1.2	11.9
7	77.6	83.5	5.9	10.6
8	95.9	80.6	5.1	14.3
9	99.8	79.5	3.8	16.7

Table-5: S/N response table for the yield of ECH.

Factor	Mean S/N ratio (dB)			
	Level 1	Level 2	Level 3	Max-min
A	-2.434	-2.835	-2.578	0.401
B	-3.406	-2.186	-2.256	1.220
C	-1.425	-2.163	-4.259	2.834
The total mean S/N ratio $\overline{\eta}$ = -2.771 dB.				

Analysis of variance

The analysis of variance (ANOVA) is intended for sorting three process factors according to their influences to the quality characteristic. To fulfill the analysis, by estimating the sum of the squares of the S/N ratio, the total variability can be measured, which was required to be separated from the total mean S/N ratio, aimed to reach the contributions of each experimental factors and the error to final product yield [23, 24]. Firstly, SS_T, totalizing squared deviations from the total mean S/N ratio $\overline{\eta}$, can be calculated as Eq. (5).

$$SS_T = \sum_{i=1}^{K}(\eta_i - \bar{\eta})^2 \qquad (5)$$

where k is noted as number of experiments and η_i represents the S/N ratio in the orthogonal array. Meanwhile, SS_p and SS_e, which was obtained via decomposing the total sum of square deviation, Indicates each factor's sum of squared deviation and its squared error. Below is a formula for calculating factor p's SS_p,

$$SS_P = t \cdot \sum_{i=1}^{q}(\overline{\eta_{p,i}} - \bar{\eta})^2 \qquad (6)$$

where t is the repetitions of each level of the orthogonal factor, q is the number of levels, and $\overline{\eta}_{p,i}$ means the mean S/N ratio at level i.

A tool named F-test was used to find out which parameters have a more important impingement on the quality characteristic [23, 24]. For the F-test, there is a first step of computing the SS_p of each factor. MS_p is determined by dividing SS_p by the number of freedom degrees associated with the factor, df_p (number of levels minus one). Then, factors with similar MS_p to error need to be pooled to the error factor. The F-test value for each factor is defined as the ratio of the mean of squared deviation, MS_p, to the mean of squared pooled error, MS_e. Process factors with a larger F-test value have a tendency to correspond to be more vulnerable to the quality characteristic. Additionally, the percentage contributions for important factors, ρ_P can be calculated from

$$\rho_p = \frac{SS_p'}{SS_T} \cdot 100\% = \frac{SS_P - MS_e \cdot df_p}{SS_T} \cdot 100\% \qquad (7)$$

in which SS_P' means the pure sum of squared deviation of each factor.

The results of ANOVA for the designed experiment were shown in Table 6. It can be concluded that reaction time plays the most significant role in affecting the yield of ECH due to the reaction process needs sufficient time for the reactant molecules to be captured by the active sites (framework Ti). The second one is the reaction temperature: catalysis for the main reaction is enhanced at higher temperatures.While the change of molar ratio of H_2O_2 to AC results in little effect on the yield of ECH probably because of the balance kept between catalytic active centers (Ti-OOH) and the side reaction, which is more likely to occur under high H_2O_2 concentration [19].

Confirmation experiment

Since the process factors have been optimized to idealized level, the confirmation experiments are then required to be conducted as prediction and verification of the improvement caused in the yield of ECH under the optimal process condition levels [23, 24]. Eq. (8) takes η_{opt} as an estimation for the S/N ratio at the optimal the process level,

$$\eta_{opt} = \bar{\eta} + \sum_{p=1}^{0}(\overline{\eta_{p,opt}} - \bar{\eta}) \qquad (8)$$

where $\overline{\eta}$, $\overline{\eta}_{p,opt}$, o stand for the total mean S/N ratio, the mean S/N ratio for parameter p at its optimal level and the number of process factors designed in the experiment affecting the quality characteristic, separately. Obeying the equation above, prediction of the ECH yield for the optimized parameter levels can be acquired through Eq. (2) and Eq. (3).

Table-6: Analysis of variance for the yield of ECH.

Factor	Sum of squares	Degrees of freedom	Mean square	F-test	Pure sum of squares	Percentage contribution (%)
A	1.666	2	0.833	9.917	1.498	31.85
B	2.703	2	1.352	16.095	2.535	53.90
C	0.053	2	0.027	–	–	–
Error	0.281	2	0.141			
(Error)	(0.334)	(4)	0.084		(0.67)	(14.25)
Total	4.703	8			4.703	100

The variance of factor C (with open circle) is pooled into the error factor.

Table-7 compared the experimental yield of ECH with the predicted one at the optimal process parameter level. The verification experiments were executed under the optimization conditions three times. The mean yield of ECH was relatively high reaching the value of 83.13±1.03%. Gao et al obtained the ECH with the value of yield less than 75% after reacting 120 min. Lin et al obtained the similar yield of ECH under the same temperature. In addition, the yield of ECH at the optimized condition levels is the highest compared to the yield value listed in Table 3. For example, take the case of no.1, the S/N ratio (-3.832) increased by 2.227 dB to the optimal actual data (-1.605), which means that the yield of ECH had a boost about 1.29 times. Based on all results above, it can be confirmed that the prior experiment design and analysis for optimizing the reaction parameters were rational. Benefiting from Taguchi design in the synthetic process, the yield of ECH is exceedingly elevated by the reaction parameters optimization. It should be noted that, in this study, the optimal levels obtained for the reaction temperature and molar ratio of H_2O_2 to AC are both at the lowest levels, implying that quality characteristic might be further optimized if further experiments were designed and carried out. Therefore, optimizing process factors is a crucial part of increasing ECH yield during the synthesis process.it can be concluded that during the synthesis process, optimizing process factors is a crucial component of improving the ECH yield. Furthermore, most of literatures [18, 37, 38] only discussed the effect of single factor (e.g., temperature, reaction time, different solvents) on the yield or selectivity of ECH, but no analysis and comparison of the interaction between various factors. In this work, 3-levels orthogonal experiment was designed by means of mathematical statistical model in order to explore the interaction between different factors, such as temperature, reaction time and Molar ratio of H_2O_2 to AC, and the influence of their interaction on the yield of ECH. After that, the better operation conditions and high yield of ECH were obtained, indicating this model could improve the experimental efficiency.

Table-7: Results of the confirmation experiment.

	Experiment		Prediction	
Optimal	Yield (%)	S/N ratio	Yield	S/N ratio
A1B2C3	83.13±1.03%	-1.605	82.4%	-1.636

[a] Standard uncertainty in the yield of ECH are reported following ± signs. The values are obtained at least three measurements at each condition.

Conclusion

In this paper, a number of process factors necessary to raise yields of ECH were designed and analyzed using the Taguchi method. By using the Taguchi method, the reaction parameters in ECH synthesis could be optimized using a systematic and effective methodology that required fewer experiments than other optimization methods. Optimizing the synthetic factors led to a significant improvement in ECH yield as demonstrated in this study. The optimal parameter levels are reaction temperature of 40 °C, reaction time of 90 min, and molar ratio of H_2O_2 to AC equal to 1. Additionally, the results of ANOVA revealed that the reaction time is the weightiest synthesis variable affecting the yield of ECH, after which comes the reaction temperature. The variation of molar ratio of H_2O_2 to AC had bare effect on the yield of ECH. In the end, a confirmation experiment was treated to ensure that the predicted yield was valid.

References

1. R. C. Klingender, Polyepichlorohydrin Elastomer. In Handbook of Specialty Elastomers, CRC Press: Boca Raton, FL, p. 245 (2008).
2. K. Owens, and V. Kyllingstad, Elastomers, Synthetic Polyether. In Kirk-Othmer Encyclopedia of Chemical Technology, John Wiley & Sons, New York, p. 1080 (1995).
3. M. I. Childers, J. M. Longo, N. J. Van Zee, A. M. LaPointe, and G. W. Coates, Stereoselective Epoxide Polymerization and Copolymerization, *Chem. Rev*, **114**, 8129 (2014).
4. M. Wang, Y. She, X. Zhou, and H. Ji, Efficient Solvent-free Synthesis of Chloropropene Carbonate from the Coupling Reaction of CO_2 and Epichlorohydrin Catalyzed by Magnesium Porphyrins as Chlorophyll-like Catalysts, *Chinese J. Chem. Eng.*, 19, 446(2011).
5. K. Weissermel, H. Arpe, Industrial Organic Chemistry, John Wiley & Sons, New York, p.300 (2008)
6. M. Wang, Y. B. She, X. T. Zhou and H. B. Ji, Efficient Solvent-free Synthesis of Chloropropene Carbonate from the Coupling Reaction of CO_2 and Epichlorohydrin Catalyzed by Magnesium Porphyrins as Chlorophyll-like Catalysts, *Chinese J. Chem. Eng.*, **19**, 446(2011).
7. P. Hota, M. Miah, A. Gupta, D. Chakravorty and S. K. Saha, Epichlorohydrin Functionalized Graphene Oxide for Superior Li^+ Ion Conduction and Supercapacitor Application, *Mater. Chem. Phys*, **223**, 447(2019).

8. G. W. Yang, C. K. Xu, R. Xie, Y. Y. Zhang, X. F. Zhu and G. P. Wu, Pinwheel-Shaped Tetranuclear Organoboron Catalysts for Perfectly Alternating Copolymerization of CO_2 and Epichlorohydrin, *J. Am. Chem. Soc.*, **143**, 3455 (2021).

9. G. M. Lari, G. Pastore, C. Mondelli and J. Pérez-Ramírez, Towards Sustainable Manufacture of Epichlorohydrin from Glycerol Using Hydrotalcite-derived Basic Oxides, *Green Chem.*, **20**, 148(2018).

10. E. Santacesaria, R. Tesser, M. Di Serio, L. Casale and D. Verde, New Process for Producing Epichlorohydrin via Glycerol Chlorination, *Ind. Eng. Chem. Res.*, **49**, 964 (2010).

11. S. M. Danov, A. V. Sulimov and A. V. Ovcharova, Modeling of the Vapor-Liquid Equilibrium in the System Formed by the Epichlorohydrin Synthesis Products, *Theor. Found. Chem. Eng.*, **46**, 31 (2012).

12. L. L. Wang, Y. M. Liu, W. Xie, H. J. Zhang, H. H. Wu, Y. W. Jiang, M. Y. He and P. Wu, Highly Efficient and Selective Production of Epichlorohydrin through Epoxidation of Allyl Chloride with Hydrogen Peroxide over Ti-MWW Catalysts, *J. Catal.*, **246**, 205-214 (2007).

13. B. M. Bell, J. R. Briggs, R. M. Campbell, S. M. Chambers, P. D. Gaarenstroom, J. G. Hippler, B. D. Hook, K. Kearns, J. M. Kenney, W. J. Kruper, D. J. Schreck, C. N. Theriault, and C. P. Wolfe, Glycerin as a Renewable Feedstock for Epichlorohydrin Production. The GTE process. *CLEAN-Soil Air Water*, **36**, 657 (2008).

14. S. J. Wang, D. S. H. Wong, I. J. Q. Lim, Y.T. Chen and C.C. Huang, Design and Control of a Novel Plant-Wide Process for Epichlorohydrin Synthesis by Reacting Allyl Chloride with Hydrogen Peroxide, *Ind. Eng. Chem. Res.*, **57**, 6926 (2018).

15. C. C. Huang, S. J. Wang, and D. S. Wong, Design and Control of a Plant-Wide Process for the Production of Epichlorohydrin, *6th International Symposium on Advanced Control of Industrial Processes* (AdCONIP). IEEE, **2017**, 383 (2017).

16. C.B. Dartt and M.E. Davis, Applications of Zeolites to Fine Chemicals Synthesis, *Catal. Today*, **19**, 151 (1994).

17. J. Li, G. D. Zhao, S. Gao, Y. Lv, J. Li and Z. W. Xi, Epoxidation of Allyl Chloride to Epichlorohydrin by A Reversible Supported Catalyst with H_2O_2 under Solvent-Free Conditions, *Org. Process Res. Dev.*, **10**, 876(2006).

18. R. K. Pandey and R. Kumar, Eco-Friendly Synthesis of Epichlorohydrin Catalyzed by Titanium Silicate (TS-1) Molecular Sieve and Hydrogen Peroxide, *Catal. Commun.*, **8**, 379(2007).

19. G. Q. Wu, Z. G. Lin, L. Li, L. Zhang, Y. Hong, W. Wang, C. Chen, Y. Jiang and X. Yan, Experiments and Kinetics of the Epoxidation of Allyl Chloride with H_2O_2 over Organic Base Treated TS-1 Catalysts, *Chem. Eng. J.*, **320**,1 (2017).

20. T. Guo, B. R. Wang, X. Peng, M. Lin, B. Zhu, Y. Zhang, C. Xia, W. Liao and X. Shu, Enhanced Activity of Hierarchical TS-1 Synthesized via Tuning Porosity and Titanium Coordination, *Ind. Eng. Chem. Res.*, **58**, 7892(2019).

21. Z. Song, X. Feng, N. Sheng, D. Lin, Y. Li, Y. Liu, X. Chen, X. Zhou, D. Chen, and C. Yang, Propene Epoxidation with H_2 and O_2 on Au/TS-1 Catalyst: Cost-effective Synthesis of Small-sized Mesoporous TS-1 and Its Unique Performance, *Catal. Today*, 347, 102(2020).

22. T. Iwasaki, M. Isaka, H. Nakamura, M. Yasuda, S. Watano, Synthesis of Titanosilicate TS-1 Crystals via Mechanochemical Route using Low Cost Materials, *Micropor. Mesopor. Mat.*, 150, 1 (2012).

23. G. Taguchi, Quality Engineering in Japan, *Commun. Stat-Theor M.*, **14**, 2785 (1985).

24. D.C. Montgomery, Design and analysis of experiments, John Wiley & Sons, New York, p. 570(2017).

25. F. Googerdchian, A. Moheb, R. Emadi, and M. Asgari, Optimization of Pb (II) Ions Adsorption on Nanohydroxyapatite Adsorbents by Applying Taguchi Method. *J. Hazard. Mater.*, **349**, 186(2018).

26. E. R. Fitzharris, I. Watt, D. W. Rosen, and M. L. Shofner, Interlayer Bonding Improvement of Material Extrusion Parts with Polyphenylene Sulfide Using the Taguchi Method. *Addit. Manuf.*, **24**, 287(2018).

27. K.T. Matin, D. Bastani and H. Kazemian, Applying the Taguchi Method to Develop an Optimized Synthesis Procedure for Nanocrystals of T-Type Zeolite, *Chem. Eng. Technol.*, **32**, 1042(2009).

28. O. N. Ata, M. Yeşilyurt, S. Çolak and A.V. Beşe, Determination of the Optimum Conditions for Zinc Extraction from Ore Containing Sphalerite by HCl Solutions, *Can. J. Chem. Eng.*, **80**, 1 (2002).

29. Y. Zuo, X. Wang, and X. Guo, Synthesis of Titanium Silicalite-1 with Small Crystal Size by Using Mother Liquid of Titanium Silicalite-1 as Seed. *Ind. Eng. Chem. Res.*, **50**, 8485(2011).

30. M. Wang, J. Zhou, G. Mao, and X. Zheng, Synthesis of TS-1 from an Inorganic Reactant System and Its Catalytic Properties for Allyl

Chloride Epoxidation, *Ind. Eng. Chem. Res.*, **51**, 12730 (2012).

31. R. B. Khomane, B. D. Kulkarni, A. Paraskar and S.R. Sainkar, Synthesis, Characterization and Catalytic Performance of Titanium Silicalite-1 Prepared in Micellar Media. *Mater. Chem. Phys.*, **76**, 99 (2002).

32. Q.H. Xia and Z. Gao, Crystallization Kinetics of Pure TS-1 Zeolite Using Quaternary Ammonium Halides as Templates, *Mater. Chem. Phys.*, **47**, 225 (1997).

33. Y. Wang, Y. Chang, M. Liu, A. Zhang and X. Guo, A facile Strategy to Prepare Shaped ZSM-5 Catalysts with Enhanced Para-Xylene Selectivity and Stability for Toluene Methylation: The Effect of in situ Modification by Attapulgite. *Molecules*, **24**, 3462(2019).

34. C.S. Cundy and J.O. Forrest, Some Observations on the Preparation and Properties of Colloidal Silicalites: Part II: Preparation, Characterisation and Properties of Colloidal Silicalite-1, TS-1, Silicalite-2 and TS-2, *Micropor. Mesopor. Mat.*, **72**, 67(2004).

35. I. Rasaee, M. Ghannadnia and S.Baghshahi, Biosynthesis of Silver Nanoparticles using Leaf Extract of Satureja Hortensis Treated with NaCl and Its Antibacterial Properties, *Micropor. Mesopor. Mat.*, **264**, 240 (2018).

36. V. Štengl, D. Králová, F. Opluštil, and T. Němec, Mesoporous Manganese Oxide for Warfare Agents Degradation, *Micropor. Mesopor. Mat.*, **156**, 224(2012).

37. H. Gao, G. Lu, J. Suo and S. Li, Epoxidation of Allyl Chloride with Hydrogen Peroxide Catalyzed by Titanium Silicalite 1, *Appl. Catal. A: Gen.*, **138**, 27 (1996).

38. W. Feng, Y. Wang, G. Wu, Y. Lin, J. Xu, H. Shi, T. Zhang, S. Wang, X. Wu and P. Yao, Liquid Phase Propylene Epoxidation with H_2O_2 on TS-1/SiO_2 Catalyst in a Fixed-Bed Reactor: Experiments and Deactivation Kinetics, *J. Chem. Technol. Biot.*, **90**, 1489 (2015).